



Expression of a novel type of KMT2A/EPS15 fusion transcript in FLT3 mutation-positive B-lymphoblastic leukemia with t(1;11)(p32;q23)

Yamamoto, Katsuya ; Yakushijin, Kimikazu ; Mizutani, Yu ; Okuni-Watanabe, Marika ; Goto, Hideaki ; Higashime, Ako ; Miyata, Yoshiharu ...

(Citation)

Cancer Genetics, 254:92-97

(Issue Date)

2021-06

(Resource Type)

journal article

(Version)

Accepted Manuscript

(Rights)

© 2021 Elsevier Inc.

This manuscript version is made available under the CC-BY-NC-ND 4.0 license

<http://creativecommons.org/licenses/by-nc-nd/4.0/>

(URL)

<https://hdl.handle.net/20.500.14094/90008353>



Expression of a novel type of *KMT2A/EP315* fusion transcript in *FLT3* mutation-positive B-lymphoblastic leukemia with t(1;11)(p32;q23)

Katsuya Yamamoto ^a, Kimikazu Yakushijin ^a, Yu Mizutani ^a, Marika Okuni-Watanabe ^a,
Hideaki Goto ^a, Ako Higashime ^a, Yoshiharu Miyata ^a, Akihito Kitao ^a, Hisayuki Matsumoto
^b, Jun Saegusa ^b, Hiroshi Matsuoka ^a, Hironobu Minami ^a

^a *Division of Medical Oncology/Hematology, Department of Medicine, Kobe University
Graduate School of Medicine, Kobe, Japan*

^b *Department of Clinical Laboratory, Kobe University Hospital, Kobe, Japan*

Running title: Novel *KMT2A/EP315* in ALL with t(1;11)

Word count: 2440

Corresponding author: Katsuya Yamamoto

Address: Division of Medical Oncology/Hematology, Department of Medicine, Kobe University Graduate School of Medicine, 7-5-1 Kusunoki-cho, Chuo-ku, Kobe 650-0017, Japan

TEL: +81-78-382-5820

FAX: +81-78-382-5821

E-mail: kyamamo@med.kobe-u.ac.jp

Abstract

The t(1;11)(p32;q23) translocation is a rare but recurrent cytogenetic aberration in acute myeloid leukemia (AML) and B-cell acute lymphoblastic leukemia (B-ALL). This translocation was initially shown to form a fusion gene between *KMT2A* exon 8 at 11q23 and *EP315* exon 2 at 1p32 in AML. Activating mutations of *FLT3* are frequently found in AML but are very rare in ALL. Here, we describe a 75-year-old woman who was diagnosed with B-ALL since her bone marrow was made up of 98.2% lymphoblasts. These blasts were positive for CD19, CD22, CD79a, CD13, and CD33 but negative for CD10 and myeloperoxidase. The karyotype by G-banding and spectral karyotyping was 46,XX,t(1;11)(p32;q23). Expression of *KMT2A/EP315* and reciprocal *EP315/KMT2A* fusion transcripts were shown: *KMT2A* exon 8 was in-frame fused to *EP315* exon 12, indicating that this fusion transcript was a novel type. Considering three reported B-ALL cases, *EP315* breakpoints were markedly different between AML (exon 2) and B-ALL (exons 10-12). Furthermore, an uncommon type of *FLT3* mutation in the juxtamembrane domain was detected: in-frame 4-bp deletion and 10-bp insertion. Accordingly, our results indicate that the novel type of *KMT2A/EP315* fusion transcript and *FLT3* mutation may cooperate in the pathogenesis of adult B-ALL as class II and class I mutations, respectively.

Keywords: B-lymphoblastic leukemia, *KMT2A/EP315*, *FLT3* mutation

Introduction

The *KMT2A* gene (alias *MLL*) encodes a large protein (431 kDa) that possesses histone methyltransferase activity on histone H3 lysine 4 and activates the expression of posterior *HOXA* genes in the hematopoietic cell lineage [1]. *KMT2A* is located on 11q23 and is implicated in the pathogenesis of acute myeloid leukemia (AML) and acute lymphoblastic leukemia (ALL) through the formation of fusion genes with more than 70 partners by reciprocal chromosomal translocations, deletions, and inversions [1,2]. These rearrangements usually connect the 5' portion of *KMT2A* with the 3' portion of corresponding partner genes on derivative 11 chromosomes. The t(1;11)(p32;q23) translocation is a rare but recurrent cytogenetic aberration observed in AML (especially in M4 and M5 according to French–American–British criteria) and B-ALL [3,4]. Molecular cloning initially identified the fusion gene between *KMT2A* exon 8 and the *EP315* (epidermal growth factor receptor pathway substrate 15) gene exon 2 in three cases of AML with t(1;11)(p32;q23) [5,6]. *EP315* is located at 1p32 and encodes a cytoplasmic phosphoprotein that was originally discovered as a substrate of the epidermal growth factor receptor tyrosine kinase. Furthermore, different types of *KMT2A/EP315* fusion transcripts were identified in three B-ALL cases [7-10]. The resultant *KMT2A/EP315* fusion protein is thought to contribute to leukemic transformation by *HOX* gene activation and the enhanced self-renewal of hematopoietic progenitors [11].

The *FLT3* gene encodes a transmembrane receptor tyrosine kinase that is normally expressed in hematopoietic stem or progenitor cells. Activating mutations of *FLT3* are found in approximately 30% of newly diagnosed AML cases. They occur as either internal tandem duplications (ITD) in the juxtamembrane domain (~25%) or point mutations in the tyrosine kinase domain (TKD) (7–10%) [12]. Both mutations constitutively activate *FLT3* kinase activity, leading to proliferation and survival of leukemic cells. However, these *FLT3* muta-

tions are very rare in ALL [13,14]. Here, we describe an unusual case of B-ALL with t(1;11)(p32;q23) that demonstrated a novel type of *KMT2A/EP315* fusion transcript and an uncommon type of *FLT3* mutation in the juxtamembrane domain.

Material and methods

Case history

A 75-year-old woman was admitted to our hospital because of leukocytosis and the appearance of blasts in her peripheral blood. The patient had a history of Sjögren syndrome and chronic thromboembolic pulmonary hypertension, but no history of chemotherapy or radiotherapy for malignancies. She did not have any extramedullary mass, including lymphadenopathy. Peripheral blood values on admission were hemoglobin 107 g/L, platelets 81×10^9 /L and leukocytes 85.3×10^9 /L with 3% segmented neutrophils, 1% lymphocytes, and 96% blasts. Her bone marrow was hypercellular with 98.2% blasts. Medium- to large-sized blasts showed fine nuclear chromatin, a pale cytoplasm, and a lack of azurophilic granules (Fig. 1A). These blasts were negative for myeloperoxidase (MPO) and periodic acid–Schiff staining (Fig. 1B).

Immunophenotyping by three-color flow cytometry using CD45/side scatter gating revealed that gated cells (96.8% of all bone marrow cells) were positive (>20%) for CD13 (70.4%), CD19 (99.7%), CD33 (41.4%), HLA-DR (98.7%), CD22 (78.3%), CD79a (87.0%), CD38 (90.1%), and TdT (25.8%), but negative for CD10 (0.7%), CD20 (0.3%), and MPO (1.0%) (Fig. 1C). Molecular screening showed that major and minor *BCR/ABL1* fusion transcripts were negative, whereas *FLT3*-ITD seemed to be positive. An initial diagnosis of *BCR/ABL1*-negative B-lymphoblastic leukemia was made. The patient received induction therapy with a hyper-CVAD/MA regimen (cyclophosphamide, vincristine, doxorubicin,

dexamethasone, methotrexate, cytarabine), and achieved a hematological and cytogenetic complete remission (CR) after one course. She then received a further three courses of hyper-CVAD/MA as consolidation therapy and remained in CR. After 10 months, the disease relapsed: the bone marrow was made up of 90.0% lymphoblasts positive for CD19 and CD22. Salvage treatment with inotuzumab ozogamicin was performed without apparent effect. The patient died of progressive disease 13 months after the initial diagnosis.

G-banding, spectral karyotyping, and fluorescence in situ hybridization analyses

Chromosome analyses were performed using a G-banding technique on short-term cultured bone marrow cells. Karyotypes were described according to the 2016 edition of the International System for Human Cytogenetic Nomenclature. Spectral karyotyping (SKY) analysis was carried out with Sky Paint Probes (Applied Spectral Imaging, Carlsbad, CA) on five metaphase spreads. Chromosomes were counterstained with 4', 6-diaminido-2-phenylindole dihydrochloride (DAPI). We also performed fluorescence *in situ* hybridization (FISH) analyses on 20 metaphase spreads using a Vysis LSI MLL Dual Color, Break Apart Rearrangement Probe Kit (Abbott Molecular, Abbott Park, IL).

Reverse-transcription polymerase chain reaction and nucleotide sequence analyses

Total RNA was extracted from mononuclear cells in the bone marrow at diagnosis using an RNeasy Mini Kit (Qiagen, Hilden, Germany) and transcribed to cDNA using a SuperScript VILO cDNA Synthesis Kit (Invitrogen, Carlsbad, CA). To detect the *KMT2A/EPS15* fusion transcript, we designed a forward primer, KMT2A-F7 (from *KMT2A* exon 7, 5'-AGGACCGCCAAGAAAAGAAGT-3', cDNA positions 3957–3977 according to the National Center for Biotechnology Information (NCBI) reference sequence NM_005933.4), and a reverse primer, EPS15-R14 (from *EPS15* exon 14,

5'-GGGCCTGTAGTTTTTGCAGATT-3', cDNA positions 1182–1203 according to NM_001981.3). To detect the reciprocal *EPS15/KMT2A* fusion transcript, we also used another forward primer EPS15-F11 (from *EPS15* exon 11, 5'-CGACACAAAGGACTGTGGGAA-3', cDNA positions 842-862) and a reverse primer KMT2A-R9 (from *KMT2A* exon 9, 5'-CCACTCTGATCCTGTGGACT-3', cDNA positions 4212-4231).

Reverse-transcription polymerase chain reaction (RT-PCR) was carried out using an AmpliTaq GOLD 360 Master Mix (Applied Biosystems, Foster City, CA) according to the manufacturer's instructions. PCR mixtures were denatured at 95°C for 10 min and 40 cycles of PCR (denaturation at 95°C for 30 sec, annealing at 58°C for 30 sec, and extension at 72°C for 30 sec) were performed in a thermal cycler followed by a final extension at 72°C for 10 min. The PCR products were analyzed by electrophoresis on a 2.0% agarose gel using a 100-bp DNA ladder (TaKaRa, Shiga, Japan) as a size marker. Sequencing reactions were carried out using a BigDye Terminator v3.1 Cycle Sequencing Kit (Applied Biosystems) and the primers mentioned above. The sequences were analyzed on a 3500 Dx Genetic Analyzer (Applied Biosystems).

To detect the *FLT3*-ITD mutation, we used a forward primer, R5 (from *FLT3* exon 12, 5'-TGTCGAGCAGTACTCTAAACATG-3', cDNA positions 1553–1575 according to NCBI reference sequence NM_004119.3), and a reverse primer, 12R (from *FLT3* exon 15, 5'-CTTTCAGCATTTTGACGGCAACC-3', cDNA positions 1986–2008) [15]. PCR mixtures were denatured at 95°C for 10 min and 30 cycles of PCR (denaturation at 95°C for 30 sec, annealing at 60°C for 30 sec, and extension at 72°C for 30 sec) were performed in a thermal cycler followed by a final extension at 72°C for 10 min. The PCR products were analyzed by electrophoresis on a 3.0% agarose gel.

Results

Chromosome analysis of bone marrow cells on admission showed 46,XX,t(1;11)(p32;q23)[18]/46,sl,-19,+mar[1]/46,XX[1] (Fig. 1D). In hematological CR after induction therapy, the karyotype returned to 46,XX[20]. At relapse, the karyotype was 46,XX,t(1;11)(p32;q23)[13]/46,XX[7]. SKY revealed both der(1)t(1;11)(p32;q23) and der(11)t(1;11)(p32;q23) (Fig. 1E). FISH on metaphase spreads revealed that 5' *KMT2A* and 3' *KMT2A* signals were split into der(11)t(1;11) and der(1)t(1;11), respectively, in all 20 metaphase spreads (Fig. 1F). Thus, the final diagnosis was B-lymphoblastic leukemia with t(1;11)(p32;q23.3); *KMT2A*-rearranged according to the World Health Organization classification.

We performed RT-PCR for the possible detection of *KMT2A/EP315* fusion transcripts. A PCR product of 365 bp was successfully amplified in the patient's bone marrow cells only (Fig. 2A). Nucleotide sequencing of the PCR product revealed that *KMT2A* exon 8 was in-frame fused to *EP315* exon 12 (Fig. 2B). We next performed RT-PCR for the detection of a reciprocal *EP315/KMT2A* fusion transcript. A PCR product of 272 bp was amplified in the patient's bone marrow cells (Fig. 2A). Nucleotide sequencing revealed that *EP315* exon 11 was in-frame fused to *KMT2A* exon 9 (Fig. 2B).

We also examined a *FLT3*-ITD mutation by RT-PCR. In addition to a wild-type PCR product of 456 bp, a larger PCR product was detected at initial diagnosis (Fig. 2D). This larger product became negative on CR, whereas it appeared again at relapse. Nucleotide sequencing revealed that an additional band was not derived from ITD but from an in-frame deletion of 4 bp (cDNA positions 1834–1837) and an insertion of 10 bp in the *FLT3* juxtamembrane domain (Fig. 2F, 2G). This *FLT3* mutation resulted in an insertion of four amino acids (QGGD) instead of a deletion of two amino acids (F590, Y591).

Discussion

We have detected both *KMT2A/EPS15* and *EPS15/KMT2A* fusion transcripts and an *FLT3* mutation of the juxtamembrane domain in an adult patient with B-ALL harboring a rare translocation t(1;11)(p32;q23). A total of 36 cases with t(1;11)(p32;q23), including the present case, have been described in the literature to date. They included 14 cases of AML (M0, 2; M1, 2; M4, 4; M5, 6), 19 cases of ALL (B-cell, 10; not available, 9), one case of bi-phenotypic leukemia, and two cases of myelodysplastic syndrome [3,4,6,8,16]. Namely, this translocation is slightly more common in ALL than in AML. The median age was 7 years in AML versus 1 year in ALL [4]. Median survival was 15 months with a very few long-term survivors. Of these, in addition to eight cases with *KMT2A* rearrangements shown by FISH or Southern blot analyses [16-19], six cases of AML/ALL with *KMT2A/EPS15* fusion transcripts have been reported (Table 1) [5-10]. Three AML cases showed similar *KMT2A* exon 8/*EPS15* exon 2 fusion transcripts, whereas three ALL cases displayed *KMT2A* exon 10/*EPS15* exon 12 or exon 8/exon 10 fusions [8,10]. Compared with these reported cases, the present case exhibited a fusion transcript between *KMT2A* exon 8 and *EPS15* exon 12, indicating that this fusion was a novel type. The immunophenotypes of B-ALL cases were characterized by a CD19+CD10- phenotype. Furthermore, three cases showed CD13+CD33+ although there was no case that presented lineage switch. Thus, ALL with *KMT2A/EPS15* fusion transcripts may present with a myeloid antigen-positive early precursor B (pro-B) ALL phenotype.

The *KMT2A* gene has 36 coding exons, whereas the *EPS15* gene contains 25 coding exons [4]. The *KMT2A* breakpoints in *KMT2A*-rearranged AML/ALL usually spans the major breakpoint clustering region (MBR, exon 8 to exon 14). The *KMT2A* breakpoints in cases with t(1;11)(p32;q23) were almost similar (at the end of exon 8) between AML and ALL, and were included in the MBR. In contrast, *EPS15* breakpoints were markedly different be-

tween AML and ALL: exon 2, and exon 10 to 12. Therefore, the resultant KMT2A/EPS15 fusion protein in AML had the AT hook and CXXC domain of KMT2A, three Eps15 Homology (EH) domains, a coiled-coil region, a region rich in aspartate-proline-phenylalanine repeats, a proline-rich region, and ubiquitin-interacting motifs of EPS15 [4,8]. Alternatively, the fusion protein in the present case and other ALL cases lacked EH domains but retained the coiled-coil region of EPS15. As Shinohara et al. suggested, these findings indicate that EH domains may be involved in leukemic cell differentiation, and be essential to myeloid but not lymphoid leukemogenesis [8]. Our results supported this speculation as well. In fact, So et al. clearly demonstrated that coiled-coil oligomerization domains are necessary and sufficient for leukemogenic transformation induced by *KMT2A/EPS15*, whereas EH domains were neither necessary nor sufficient for *in vitro* transformation [11]. Furthermore, cells transfected with a *KMT2A* exon 8/*EPS15* exon 2 construct induced leukemias in sublethally irradiated mice. Blasts consistently displayed a surface phenotype characteristic of myeloid progenitors. Therefore, similar experiments using a *KMT2A* exon 8/*EPS15* exon 10 or 12 construct may be useful to elucidate whether this type of fusion gene could induce lymphoid leukemia.

In *KMT2A*-rearranged leukemias, the roles of reciprocal 5' partner/3' *KMT2A* fusion proteins have been poorly explained. However, reciprocal *EPS15/KMT2A* fusion transcripts were expressed in all cases examined (Table 1). Furthermore, cytogenetically, case 3 had an additional abnormality der(1)t(1;11)(p32;q23) leading to duplication of the *EPS15/KMT2A* fusion gene [6]. Thus, the reciprocal *EPS15/KMT2A* may have some role, including disease progression, in the pathogenesis of AML/ALL. Interestingly, in the other two ALL cases (cases 5 and 6), skipping of the *KMT2A* exon 9 was evident at the transcriptional level, although the *KMT2A* breakpoints were located at the end of exon 8 [10]. In contrast, the present case retained the *KMT2A* exon 9, as observed in three AML cases (cases 1 to 3). Thus, our

results indicate that skipping of *KMT2A* exon 9 does not always occur in the formation of *EP315/KMT2A* fusion transcripts in ALL.

Another noticeable finding in the present case is the *FLT3* mutation in the juxtamembrane domain at diagnosis and at relapse. Compared with AML, activating mutations of *FLT3* are rarely found in ALL. The analysis of 12 references revealed that *FLT3*-TKD mutations and *FLT3*-ITD occurred in 76/1213 (6.3%) and 12/1213 (1.0%) of childhood ALL patients, respectively [14]. With regard to *KMT2A* rearrangements, elevated *FLT3* mRNA expression levels were detected in *KMT2A*-rearranged infant ALL as compared to both infants and noninfants carrying germline *KMT2A* genes [20]. *FLT3*-TKD mutations were found in 3% (1/36), 16% (5/30), and 18% (8/44) of *KMT2A*-rearranged infant ALL cases [20-22], whereas *FLT3*-ITD in the juxtamembrane domain was not detected in these ALL cases. In contrast, *FLT3*-TKD (D835/I836) and *FLT3*-ITD mutations were not present in two ALL infants with *KMT2A/EP315* fusion transcripts (Table 1, cases 5 and 6) [10]. These findings suggest that *FLT3*-TKD mutations but not *FLT3*-ITD may have a specific association with *KMT2A* rearrangements in infant ALL as the second genetic events [22]. In the present case, instead of *FLT3*-ITD and TKD mutations, we found an uncommon type of mutation: an in-frame 4-bp deletion and a 10-bp insertion, leading to a two-amino acid elongation in the juxtamembrane domain. This type of *FLT3* mutation was previously reported in four cases of childhood ALL without *KMT2A* rearrangements: three hyperdiploid cases showed a deletion (with or without substitution) within a seven-amino acid region (Fig. 2G), and one case showed a 3-bp deletion and an 18-bp insertion [23]. As observed in the present case, two hyperdiploid cases also demonstrated deletions from F590, indicating that this region may be a recurrent deletion breakpoint in both childhood and adult ALL. An elongating or shortening juxtamembrane domain of *FLT3* was shown to induce ligand-independent receptor activation [24], indicating that the *FLT3* mutation in the present case could lead to the constitu-

tive activation of tyrosine kinases as the second genetic event in the same cells. Accordingly, our results indicate that the novel type of *KMT2A/EPS15* fusion transcript and *FLT3* mutation could cooperate in the pathogenesis of adult B-ALL by impaired differentiation (class II mutation) and by enhanced proliferation and survival (class I mutation) of progenitor cells, respectively [13].

At present, first- and next-generation FLT3 tyrosine kinase inhibitors are clinically used for AML with *FLT3* mutations [12]. In comparison, in ALL, leukemic cells from infants with *KMT2A*-rearranged ALL expressing high *FLT3* mRNA levels were shown to be more sensitive to the FLT3 inhibitor PKC412 (midostaurin) than ALL cells from noninfants. This cytotoxic response was comparable to the response observed in cells from AML with *FLT3*-ITD, although PKC412 has multitarget kinase inhibition that includes the inhibition of FLT3 [20,21]. Thus, it is interesting to investigate whether FLT3 inhibitors could be clinically useful for ALL with a *FLT3* mutation and *KMT2A* rearrangement.

Conflict of interest

All authors have no conflict of interest.

References

- [1] Yokoyama A. Molecular mechanisms of MLL-associated leukemia. *Int J Hematol* 2015;101:352-361.
- [2] Marschalek R. Mechanisms of leukemogenesis by MLL fusion proteins. *Br J Haematol* 2011;152:141-154.
- [3] Mitelman F, Johansson B, Mertens F (Eds.). *Mitelman Database of Chromosome Aberrations and Gene Fusions in Cancer* (2020). <https://mitelmandatabase.isb-cgc.org>. ac-

cessed January 15, 2020.

- [4] Huret JL. t(1;11)(p32;q23). Atlas Genet Cytogenet Oncol Haematol 2011;15:529-532.
- [5] Bernard OA, Mauchauffe M, Mecucci C, et al. A novel gene, AF-1p, fused to HRX in t(1;11)(p32;q23), is not related to AF-4, AF-9 nor ENL. Oncogene 1994;9:1039-1045.
- [6] Sagawa M, Shimizu T, Shimizu T, et al. Establishment of a new human acute monocytic leukemia cell line TZ-1 with t(1;11)(p32;q23) and fusion gene *MLL-EPS15*. Leukemia 2006;20:1566-1571.
- [7] Ueda K, Yamamoto G, Shinohara A, et al. Early onset of acute lymphoblastic leukemia with MLL rearrangement after autologous stem cell transplantation for multiple myeloma. Ann Hematol 2009;88:813-814.
- [8] Shinohara A, Ichikawa M, Ueda K, et al. A novel MLL-AF1p/Eps15 fusion variant in therapy-related acute lymphoblastic leukemia, lacking the EH-domains. Leuk Res 2010;34:e62-e63.
- [9] Kotecha RS, Murch A, Kees U, et al. Pre-natal, clonal origin of t(1;11)(p32;q23) acute lymphoblastic leukemia in monozygotic twins. Leuk Res 2012;36:46-50.
- [10] Kotecha RS, Ford J, Beesley AH, et al. Molecular characterization of identical, novel *MLL-EPS15* translocation and individual genomic copy number alterations in monozygotic infant twins with acute lymphoblastic leukemia. Haematologica 2012;97:1447-1450.
- [11] So CW, Lin M, Ayton PM, et al. Dimerization contributes to oncogenic activation of MLL chimeras in acute leukemias. Cancer Cell 2003;4:99-110.
- [12] Dayer N, Schlenk RF, Russell NH, et al. Targeting *FLT3* mutations in AML: review of current knowledge and evidence. Leukemia 2019;33:299-312.
- [13] Gilliland DG, Griffin JD. The roles of FLT3 in hematopoiesis and leukemia. Blood 2002;100:1532-1542.

- [14] Kabir NN, Rönstrand L, Kazi JU. FLT3 mutations in patients with childhood acute lymphoblastic leukemia (ALL). *Med Oncol* 2013;30:462.
- [15] Kiyoi H, Naoe T, Yokota S, et al. Internal tandem duplication of *FLT3* associated with leukocytosis in acute promyelocytic leukemia. *Leukemia* 1997;11:1447-1452.
- [16] Tsujioka T, Wada H, Yamamori S, et al. *MLL/AF-1p* fusion in therapy-related early pre-B acute lymphoblastic leukemia with t(1;11)(p32;q23) translocation developing in the relapse phase of acute promyelocytic leukemia. *Int J Hematol* 2003;78:439-442.
- [17] Harrison CJ, Cuneo A, Clark R, et al. Ten novel 11q23 chromosomal partner sites. *Leukemia* 1998;12:811-822.
- [18] Douet-Guilbert N, Morel F, Le Bris MJ, et al. Rearrangement of the *MLL* gene in acute myeloblastic leukemia: report of two rare translocations. *Cancer Genet Cytogenet* 2005;157:169-174.
- [19] De Braekeleer E, Meyer C, Douet-Guilbert N, et al. Identification of *MLL* partner genes in 27 patients with acute leukemia from a single cytogenetic laboratory. *Mol Oncol* 2011;5:555-563.
- [20] Stam RW, den Boer ML, Schneider P, et al. Targeting FLT3 in primary *MLL*-gene-rearranged infant acute lymphoblastic leukemia. *Blood* 2005;106:2484-2490.
- [21] Armstrong SA, Kung AL, Mabon ME, et al. Inhibition of FLT3 in MLL: Validation of a therapeutic target identified by gene expression based classification. *Cancer Cell* 2003;3:173-183.
- [22] Taketani T, Taki T, Sugita K, et al. *FLT3* mutations in the activation loop of tyrosine kinase domain are frequently found in infant ALL with *MLL* rearrangements and pediatric ALL with hyperdiploidy. *Blood* 2004;103:1085-1088.
- [23] Armstrong SA, Mabon ME, Silverman LB, et al. FLT3 mutations in childhood acute lymphoblastic leukemia. *Blood* 2004;103:3544-3546.

- [24] Kiyoi H, Ohno R, Ueda R, et al. Mechanism of constitutive activation of FLT3 with internal tandem duplication in the juxtamembrane domain. *Oncogene* 2002;21:2555-2563.

Figure legends

Fig. 1. Morphologic, immunophenotypic, and cytogenetic findings of bone marrow cells.

(A, B) Bone marrow smears showing lymphoblasts at diagnosis of acute lymphoblastic leukemia (ALL). Medium- to large-sized lymphoblasts show fine nuclear chromatin, a pale cytoplasm, and no azurophilic granules (A, May–Grünwald–Giemsa staining, $\times 1000$).

Lymphoblasts are negative for myeloperoxidase (MPO), whereas a neutrophil is strongly positive (B, myeloperoxidase staining, $\times 1000$).

(C) Flow cytometric analysis of bone marrow cells at diagnosis of ALL by CD45/side scatter (SSC) gating. The corresponding cell percentage demarcated by the gate is 96.8%. The results of two-color analyses with CD7 and CD10, CD33 and CD2, CD19 and CD13, CD22 and CD13, CD79a and MPO, CD34 and HLA-DR, and CD3 and CD20 for the gated cells are shown. Corresponding cell percentages in each fraction are indicated.

The gated cells are positive for CD33, CD13, CD19, CD22, CD79a, and HLA-DR.

(D) G-banded karyotype of bone marrow cells at diagnosis of ALL. The karyotype is 46,XX,t(1;11)(p32;q23). Arrows indicate rearranged chromosomes.

(E) Spectral karyotyping (SKY) of metaphase spreads after spectrum-based classification (left side, reverse DAPI; right side, SKY). Only chromosomes 1 and 11 are shown. Two derivative chromosomes, der(1)t(1;11)(p32;q23) and der(11)t(1;11)(p32;q23), are shown. Arrows indicate rearranged chromosomes.

(F) Fluorescence *in situ* hybridization (FISH) with a Vysis LSI MLL Dual Color, Break Apart Rearrangement Probe Kit (Abbott Molecular, Abbott Park, IL, USA) on metaphase spreads and interphase nuclei. Arrows indicate 1) a normal 5' *KMT2A*/3' *KMT2A* fusion signal (red/green, yellow) on a normal chromosome 11, 2) a 3' *KMT2A* signal (red) on der(1)t(1;11), and 3) a 5' *KMT2A* signal (green) on der(11)t(1;11). One each of yellow, red, and green signals are also observed on an interphase nucleus (inset).

Fig. 2. Reverse transcription–polymerase chain reaction and nucleotide sequence analyses of bone marrow cells.

(A) Detection of *KMT2A/EP515* and *EP515/KMT2A* fusion transcripts by reverse transcription–polymerase chain reaction (RT–PCR) analysis. We used two primer sets:

KMT2A-F7 and *EP515*-R14 in lanes 1 and 2, and *EP515*-F11 and *KMT2A*-R9 in lanes 3 and 4. Lane M, the DNA of a 100-bp ladder as a size marker; lanes 1 and 3, bone marrow cells of the patient at diagnosis; and lanes 2 and 4, normal bone marrow cells (negative control). The PCR products of 365 bp and 272 bp are amplified only in the cells of the patient.

(B) Nucleotide and amino acid sequences surrounding the junction of *KMT2A/EP515* and *EP515/KMT2A* fusion transcripts. *KMT2A* exon 8 is in-frame fused to *EP515* exon 12. Furthermore, *EP515* exon 11 is in-frame fused to *KMT2A* exon 9. A vertical arrow indicates the breakpoint.

(C) Schematic representation of *KMT2A/EP515* and *EP515/KMT2A* fusion transcripts. White and shaded boxes represent exons of *KMT2A* and *EP515*, respectively. The locations of the primers used for RT–PCR are indicated by horizontal arrows. The numbers of exons and nucleotides are derived from the National Center for Biotechnology Information (NCBI) reference sequence.

(D) Detection of a *FLT3* transcript by RT–PCR analysis. Lane M, the DNA of a 100-bp ladder as a size marker; lanes 1–3, bone marrow cells of the patient at diagnosis (lane 1), in complete remission (CR) (lane 2) and at relapse (lane 3); and lane 4, water (negative control). The PCR products of 456 bp (wild type) and 462 bp (mutant) are amplified in the cells of the patient at initial diagnosis. Only the wild type is found on CR, whereas the mutant appears again at relapse.

- (E) Schematic representation of the *FLT3* transcript. The locations of the primers used for RT-PCR are indicated by horizontal arrows. The breakpoint of deletion and insertion is shown by a vertical arrow. The numbers of exons and nucleotides are derived from the NCBI reference sequence.
- (F) Nucleotide and amino acid sequences of *FLT3* transcripts. Mixed sequences of wild-type and mutant *FLT3* transcripts are found from cDNA position 1834.
- (G) Nucleotide and amino acid sequences of wild-type and mutant *FLT3* transcripts. The mutant shows a deletion of 4 bp (TTCT) followed by an insertion of 10 bp (CAAGGGGGAG) at position 1834. Inserted nucleotide and amino acid sequences are shown in red letters. Different *FLT3* mutations in three patients with hyperdiploid childhood ALL (ALL-12, ALL-25, ALL-24), as reported by Armstrong et al. [23], are presented below. Deletions (–) and inserted amino acid sequences are shown in red letters.

Fig. 1

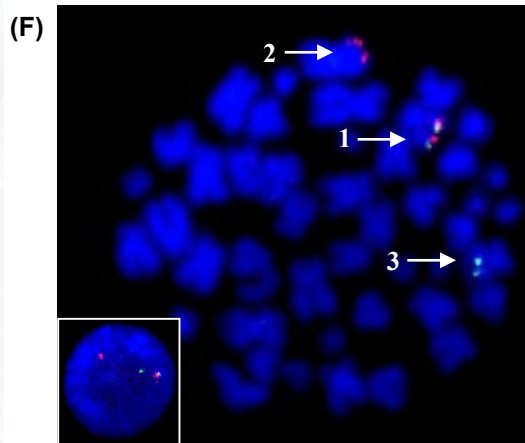
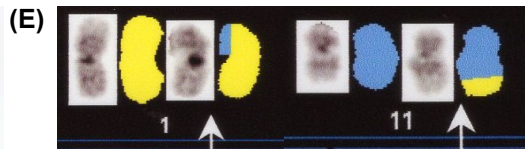
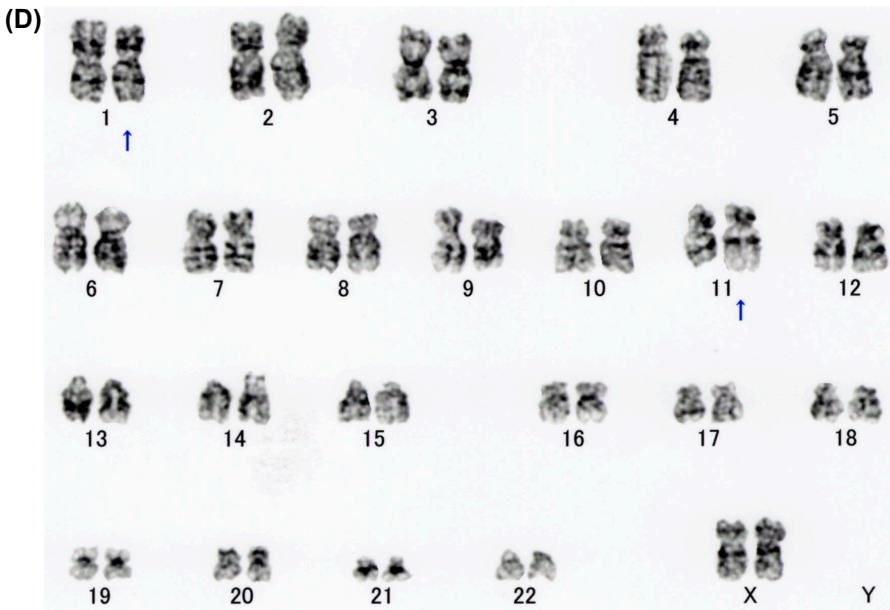
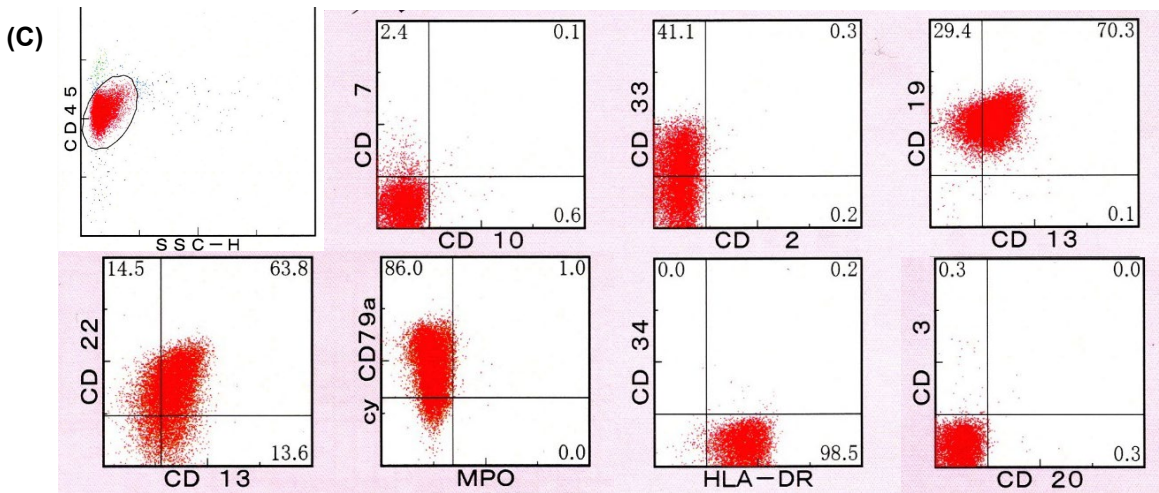
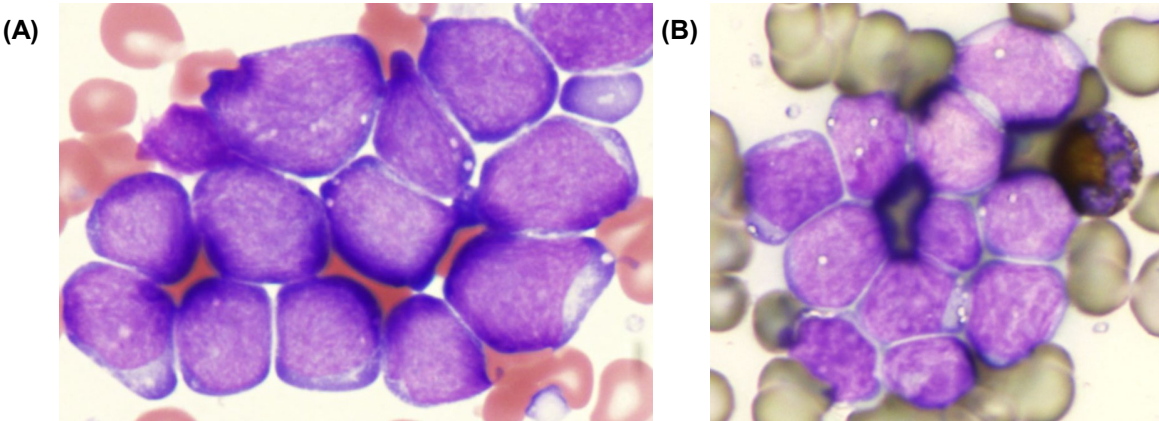


Fig. 2

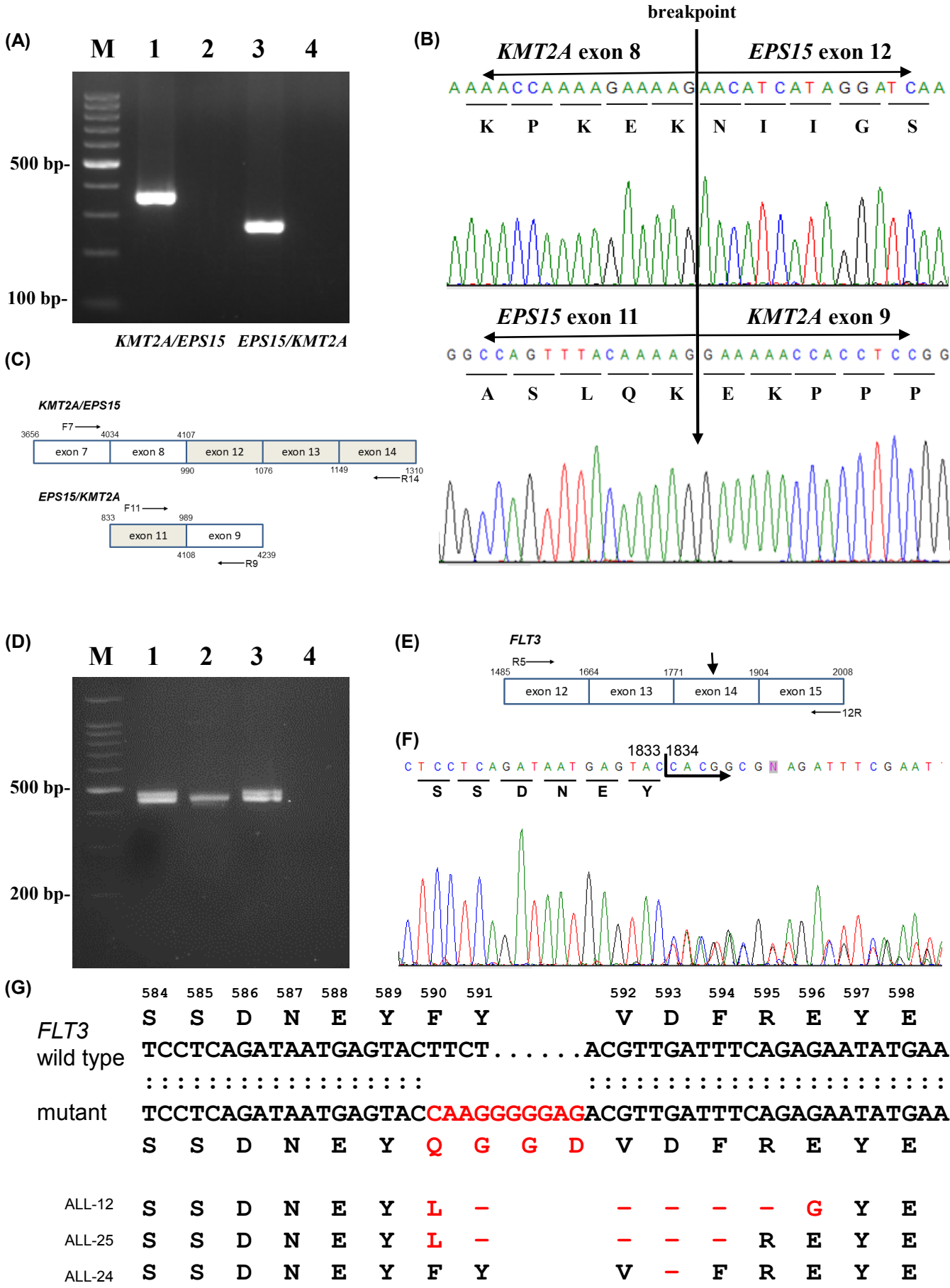


Table 1. Reported cases of hematological malignancies associated with t(1;11)(p32;q23) and *KMT2A/EPS15* fusion transcript

<i>Case No.</i>	<i>Age/ Sex</i>	<i>Dx</i>	<i>Karyotypes</i>	<i>KMT2A/EPS15 fusion trasncript</i>	<i>EPS15/KMT2A fusion transcript</i>	<i>Immunophenotypes</i>	<i>References</i>
1	4/M	AML M0	46,XY,t(1;11)(p32;q23)[11]/46,XY[1]	exon 8/exon 2	exon 1/exon 9	CD13–, CD14–, CD15+, CD19+, CD38+, DR+	[5]
2	43/F	AML M5b	46,XX,t(1;11)(p32;q23),+der(1)t(1;12)(p12;q12), -12[5]/46,XX[4]	exon 8/exon 2	exon 1/exon 9	NA	[5]
3	76/M	AML M5a	55,XY,t(1;11)(p32;q23),+der(1)t(1;11),+6,+8,+8, +13,+15,+17,+19,+21	exon 8/exon 2	exon 1/exon 9	CD13+, CD14+, CD33+, CD38+, HLA-DR+, CD7+, CD56+, CD3–, CD10–, CD19–	[6]
4	63/F	pro-B ALL	46,XX,t(1;11)(p32-34;q23)[4]/46,XX[2]	exon 10/exon 12	NA	CD19+, CD79a+, κ–, λ–	[7,8]
5	7w/F	pro-B ALL	46,XX,t(1;11)(p32;q23)[13]/ 46,XX[7]	exon 8/exon 10	exon 9/exon 10	CD19+, CD24+, CD33+, CD13+, CD10–	[9,10]
6	7w/F	pro-B ALL	46,XX,t(1;11)(p32;q23)[8]/47,sl,+X[4]/46,XX[8]	exon 8/exon 10	exon 9/exon 10	CD19+, CD24+, CD33+, CD13+, CD10–	[9,10]
7	75/F	pro-B ALL	46,XX,t(1;11)(p32;q23)[18]/46,sl,-19,+mar[1]/ 46,XX[1]	exon 8/exon 12	exon 11/exon 9	CD19+, CD13+, CD33+, HLA-DR+, CD10–, CD22+, CD79a+, MPO–	present case

Abbreviations: w, weeks; F, female; M, male; AML, acute myeloid leukemia; ALL, acute lymphoblastic leukemia; NA, not available.
The t(1;11)(p32;q23) translocation is described in bold letters.